Eur. Phys. J. D **13**, 5–10 (2001)

THE EUROPEAN PHYSICAL JOURNAL D

EDP Sciences

Spin polarization of electrons elastically scattered from europium and bismuth atoms

Neerja and A.N. Tripathi[a]

Department of physics, University of Roorkee, Roorkee 247 667, India

Received 17 February 2000 and Received in final form 15 June 2000

Abstract. We present calculations of differential, integrated elastic, total, momentum transfer cross-sections and spin-polarization parameters S, T and U for scattering of electrons from Eu and Bi atoms in the energy range 2.0 to 500.0 eV using semi-relativistic approach. The target-projectile interaction is represented both by real and complex parameter-free optical potentials in the solution of Dirac equation for the scattered electrons. The results for the differential cross-sections and spin-polarization parameters have been compared with the available calculations and experimental results.

PACS. 11.80.-m Relativistic scattering theory – 34.80.-i Electron scattering

1 Introduction

It is well-established that relativistic interactions play very crucial role in the spin-dependent phenomenon in collision between slow electrons and heavy atomic systems. Indeed these effects are so large that, even manifest themselves in the integral cross-sections in the elastic scattering from many heavier systems. In recent years, the scattering of electrons by such atoms has been studied extensively both experimentally and theoretically. It is worth mentioning that recently Anderson and Bartschat [1] have published an excellent critical review with selected examples both from experiments and theory. The older works on this subject can be traced in the classic reviews of Kessler [2] and Hanne [3].

Due to enormous progress, which has recently been achieved in the development of efficient polarized electron sources and accurate polarimeters, the spin dependence of the scattering process can be readily studied through the complete scattering experiments. Within the framework of the density matrix formalism [2,4], it is possible to define a set of observables, which describe the elastic scattering process, namely the unpolarized differential cross-section (DCS) and the S, T and U polarization parameters. The S parameter also known as Sherman function describes the change of polarization produced in the scattered beam due to collision and the other two polarization parameters T and U give the angle of rotation of the component of the polarization vector in the scattering plane.

On the theoretical side, there exits a long history for such calculations beginning with Walker [5] based on relativistic Hartree-Fock equation, Fai Lam [6] based on a relativistic form of the Schrödinger equation, Haberland and Fritsche [7] based on Kohn-Sham type equations and Bartschat *et al.* [8] using the generalized Kohn-Sham (GKS) and static exchange R-matrix theory [9]. Further, both McEachran and Stauffer [10] and Nahar and Wadehra [11] solved the relativistic form of the Schrodinger equation within the framework of model potential approach. In the former case, a hybrid way was used to calculate the scattering potential, *i.e.* its static part was obtained relativistically while the polarization potential was obtained in a non-relativistic manner. In the latter case, a real and complex model potential represents the projectile-target interaction. This approach has been successfully applied to study spin polarization in elastic scattering of electrons from a number of atoms by Kumar *et al.* [12] and Yuan and Zhang [13]. To improve the hybrid relativistic model of McEachran and Stauffer [10], Szmytkowski [14] developed a fully relativistic version of the polarized orbital approximation. This approach was used by Szmytkowski and Sienkiewicz [15] and observed that the calculated values moved in the right direction when compared to the hybrid approach. Sienkiewicz and Baylis [16] have further improved the target polarization in the relativistic version by configuration interaction procedure.

Recently Dorn *et al.* [17] carried out theoretical calculations for spin polarization for xenon atoms based on the relativistic Schrödinger equation together with an optical potential, which included both polarization and absorption effects. The comparison of their calculations with experimental data suggests that the absorption potential must be included in the relativistic description for accurate prediction of the STU parameters. This aspect has been further examined by Neerja *et al.* [18]. They have computed the spin polarization parameters STU and correlation for the electrons elastically scattered from closed shell atoms like ytterbium (Yb), radon (Rn) and radium (Ra) using an approach very similar to that of Dorn

[a] e-mail: awadhfph@isc.rurkiu.ernet.in or neerudph@isc.rurkiu.ernet.in

Table 1. Electronic configuration, term symbols, dipole polarizability, ionization potential (I.P.), first excitation potential ($E_{\rm th}$) and crossing points ($r_{\rm c}$) for Eu and Bi atoms.

Z (atomic number)	element	electronic configuration	term	polarizability (a.u.)	*I.P.* (eV)	$E_{\rm th}$ (eV)	crossing point (a.u.)
63	Eu	[Xe] $6s(2)4f(7)$	^{8}S	187.162	5.670	1.602	7.251
83	Bi	[Xe] $6s(2)4f(14)5d(10)6p(3)$	^{4}S	50.017	7.289	1.416	11.781

$$V_{\rm SR}(r) = \begin{cases} 0.0622\ln r_{\rm s} - 0.096 + 0.018\ln r_{\rm s} - 0.02 r_{\rm s}, & r_{\rm s} \le 0.7 \\ -0.1231 + 0.03796\ln r_{\rm s} & 0.7 < r_{\rm s} \le 10 \\ -0.876 r_{\rm s}^{-1} - 2.65 r_{\rm s}^{-3/2} - 2.8 r_{\rm s}^{-2} - 0.8 r_{\rm s}^{-5/2} & 10 \le r_{\rm s} \end{cases} \quad (3)$$

et al. [19]. In the present paper, we have extended our earlier calculations [12,18] to study the electron collisions with open shell elements like europium (Eu) and bismuth (Bi) atoms. Their electronic configurations in the ground states are given in Table 1.

In elastic scattering from closed-shell atoms, the polarization effects are caused by the spin-orbit interaction of the scattered electrons in the atomic field whereas from open-shell atoms that have a fine-structure splitting of their ground state, the polarization phenomenon may also be generated by the exchange interaction between the scattered and the atomic electrons along with the internal spin-orbit coupling of the atom (fine-structure effect, Hanne [3]). The present model is certainly a less good approximation for an open shell configuration like Eu and Bi atoms because it does not include the fine-structure effect. However, as it is well-known through the studies in atomic structure that within the framework of Hartree-Fock approximation, even a half-complete shell leads to a spherically symmetric equivalent potential (Bethe and Jackiw [19]), as required here. In view of this, the present model can be easily applied to study the elastic scattering from systems with open-shell atoms fulfilling this requirement. The details of theoretical methodology can be found in our previous paper [18]. Results and discussion of the present calculations are presented in Section 2, while conclusions are drawn in Section 3.

2 Results and discussion

2.1 Choice of potentials

Here the total interaction between an electron and the target atom is approximately represented by an effective potential. The real part of the potential is written as the sum of three local terms, namely the static ($V_{\rm st}$), the exchange ($V_{\rm ex}$) and the polarization ($V_{\rm pol}$) potential, which account approximately for the dynamics of the collision process. All three potential-terms *i.e.* $V_{\rm st}(r)$, $V_{\rm ex}(r)$, $V_{\rm pol}(r)$ are functions of electronic density of the target. The static potential $V_{\rm st}(r)$ and the charge density $\rho(r)$ are obtained using non-relativistic Slater type orbital of Roothann and Hartree-Fock wave functions as given by McLean and McLean [20]. In addition we have also used the compilation of the analytical function as given by Salvat *et al.* [21] which is determined by an analytical fitting procedure to Dirac-Hartree-Fock-Slater (DHFS) self-consistent data. In the present calculation, we are using the modified semi-classical exchange (MSCE) potential given by Gianturco and Scialla [22]

$$V_{\rm ex}^{\rm MSCE} = \frac{1}{2}\left[E - V_{\rm st}(r) + \frac{3}{10}(3\pi^2\rho(r))^{2/3}\right] - \frac{1}{2}\left\{\left[E - V_{\rm st}(r) + \frac{3}{10}(3\pi^2\rho(r))^{2/3}\right]^2 + 4\pi\rho(r)\right\}^{1/2}. \quad (1)$$

Realizing that the impinging electron distorts the electronic density of target which can further modify this exchange potential, *i.e.* when the polarization of the target wave-function is taken into account, we have replaced $V_{\rm st}$ in equation (1) by $V_{\rm D} = V_{\rm st} + V_{\rm pol.}$ For the polarization potential we have used a parameter-free polarization potential ($V_{\rm pol}$), which is based on the correlation energy of the target atom [23]. It has two components, the short range ($V_{\rm SR}(r)$) and the long range ($V_{\rm LR}(r)$) parts, and is given by

$$V_{\rm pot}(r) = \begin{cases} V_{\rm SR}(r) & r < r_{\rm c} \\ V_{\rm LR}(r) & r \ge r_{\rm c} \end{cases}. \quad (2)$$

Here $r_{\rm c}$ is the point where two forms cross each other for the first time. The short range form for the electron scattering with atoms is based on the free-electron gas exchange potential and is given by

see equation (3) above

where $r_{\rm s} = [3/4\pi\rho(r)]^{1/3}$ and $\rho(r)$ is the electron charge density of the target system.

The long-range form of the polarization potential is given by $V_{\rm LR}(r) = -\alpha_{\rm d}/2r^4$ where $\alpha_{\rm d}$ is the static electric dipole polarizability. The crossing point for Eu and Bi atoms along with their dipole polarizabilities, ionization potential, and first excitation thresholds are listed in Table 1.

The impact energy range considered in the present calculation exceeds the threshold energy of the inelastic electron scattering from the target systems under investigation and hence causes an absorption in the scattered

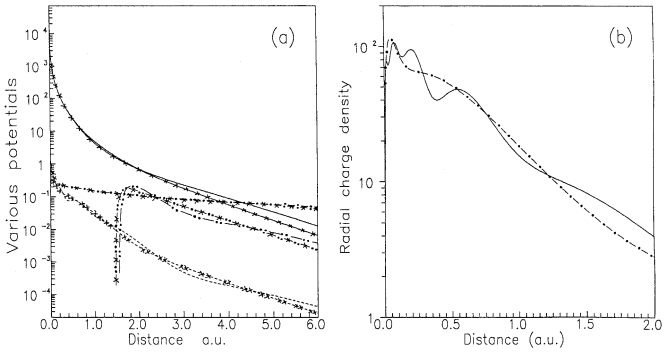

Fig. 1. (a) The negative of various components of the interaction potential for scattering of e-Eu. Present calculations: (——) static potential; (— · — ·) correlation polarization potential; (- - - -) MSCE at 100 eV; (— ·· — ··) absorption potential at 100 eV, using HF wave function [20], (—⋆—⋆—⋆—) static potential; (—⋆— · —⋆—) correlation polarization potential; (--⋆—-⋆–) MSCE at 100 eV; (—⋆— ·· —⋆—) absorption potential at 100 eV, using screening function DHFS [21]. (b) Spherical charge density of the Eu atom. Present calculation: (——) using HF wave function [20]; (— · — ·) using screening function DHFS [21].

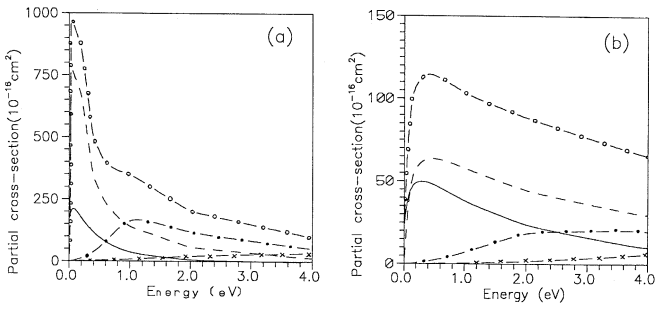

Fig. 2. Partial cross-sections in units of 10^{-16} cm^2 for scattering of (a) e-Eu, (b) e-Bi. Present calculations: (——) s-wave; (– – –) p-wave; (— · — · —) d-wave; (— × — ×) f-wave; (— ○ — ○ —) integral cross-section.

beam. There exist various versions of the absorption potential describing all the inelastic processes during the scattering. To include the absorption effect in the scattered beam, we have therefore employed a modified version 3 of the semi-empirical model absorption potential of Staszewska *et al.* [24]. It is given by

$$V_A = -\frac{1}{2} v_{\rm loc}(r)\overline{\sigma_{\rm b}}, \tag{4}$$

$$v_{\rm loc} = [2(E - V_{\rm R})]^{1/2}. \tag{5}$$

In equations (4, 5) $v_{\rm loc}$ is the local velocity of the incident electron for $E - V_{\rm R} \geq 0$, $V_{\rm R}$ is the real part of the total interaction potential, *i.e.* $V_{\rm R} = V_{\rm st} + V_{\rm ex} + V_{\rm pol}$. The factor 1/2 in equation (4) is introduced to account for the exchange of the incident electron and the bound electrons of the target during the scattering process. $\overline{\sigma_{\rm b}}$ is the average quasifree binary collision cross-section obtained non-empirically by using the free-electron gas model for the target. We avoid repeating the expressions, which are given in [24]. It is perfectly in order to point out here that the various versions of the absorption potential differ by varying $v_{\rm loc}$ and its variants. For example Staszewska *et al.* use $V_{\rm R} = V_{\rm st} + V_{\rm ex}$ for calculating $v_{\rm loc}$ in their original version referred here as version 2.

In the present work, a large number of phase shifts depending on the impact energy were evaluated before using the Born approximation. For example, the typical value of exact partial waves corresponding to the impact energies 2.0 eV and 500.0 eV is 20 and 100, respectively. Since at large distance, the interaction is dominated by the long-range part of the polarization potential $\approx -\alpha_{\rm d}/2r^4$, the Born phase shift and related scattering parameters are obtained using this term only [11,25].

2.2 Radial shapes

The various components of the interaction terms and charge density as obtained using the non-relativistic HF wave function of McLean and McLean [20] are displayed in Figures 1a and 1b for e-Eu respectively as a test case. In general, it is seen that the static interaction dominates over all other interactions (*i.e.* exchange and polarization) at small values of r ($r \approx 4$ a.u.) and thereafter the correlation polarization takes over both the static and exchange interactions. The energy dependent exchange interaction MSCE (at $E = 100$ eV) remains weaker than the static interaction up to very large r-values. We see that the absorption effects exist only in the outer region of the target and the range of $V_{\rm abs}$ is not as large as that of the polarization potential. Figure 1b shows our radial electronic charge density for Eu atom using both HF and DHFS wave function respectively. The number of peaks exhibited by the charge density curve of atoms indicates various shell contributions associated with atoms. The calculated density as obtained using the analytical fitting procedure to DHFS data as given by Salvat *et al.* [21] shows a reasonable agreement with the Hartree-Fock results. It is noted that the analytical density curve only partially reproduces the oscillations of the non-relativistic density associated with different shell contributions. Theoretical shapes of various terms of the potential and density for Bi are quite similar in nature.

2.3 Partial cross-sections in the low energy region (E < 10 eV)

We have performed calculations in different models, which are abbreviated as follows: S, static only; SE, S plus the MSCE; SEP, SE plus the correlation polarization potential; SEPa, SEP plus the absorption potential (version 3). In the present study we report our calculation in SEP and SEPa models as obtained using McLean and McLean [20] HF wave functions.

In Figures 2a and 2b, we show our results for first four partial cross-sections, for the s, p, d and f waves in SEPa approximation for Eu and Bi atoms. For Eu, as can be seen from the figure, in low energy region < 3 eV, the main contribution to the $\sigma_{\rm el}$ comes from p- and d-wave

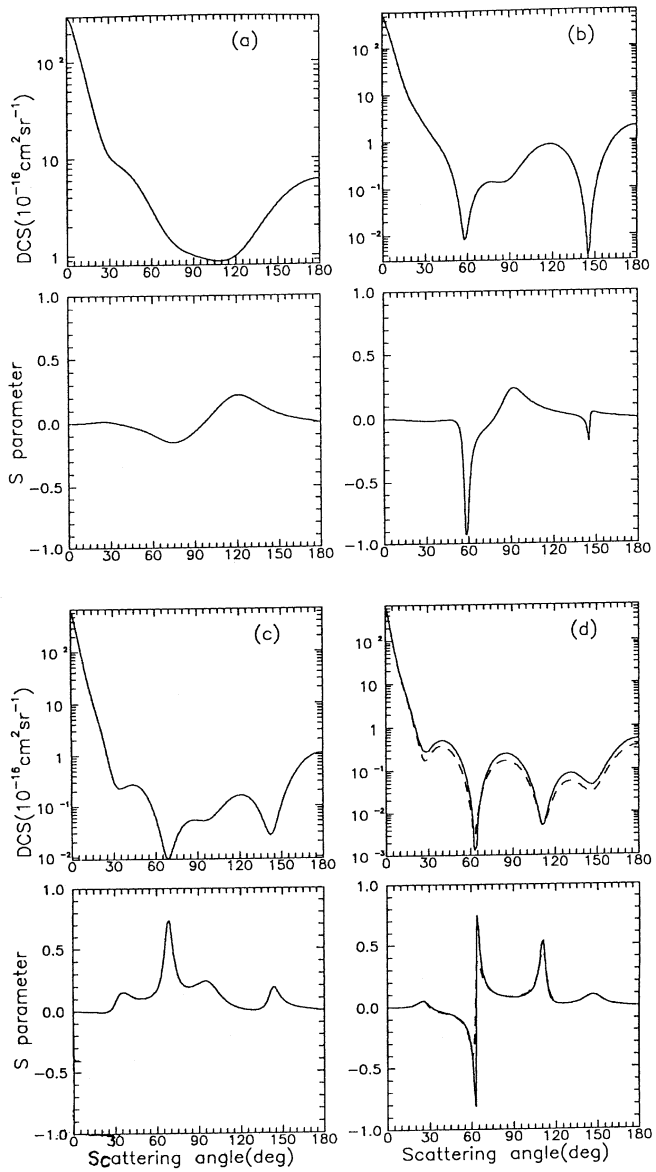

Fig. 3. Differential cross-section and spin polarization S parameter for e-Eu scattering at: (a) 10.0 eV, (b) 50.0 eV, (c) 100.0 eV, (d) 200.0 eV. Present calculations: (——) with real potential; (— — —) with complex potential.

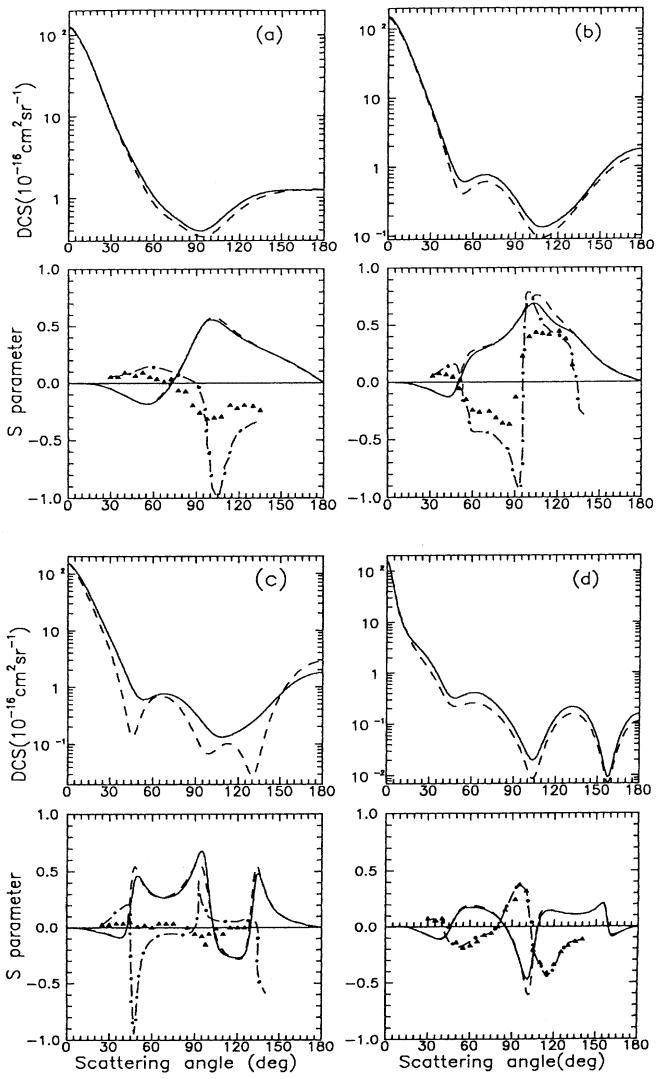

Fig. 4. Differential cross-section and spin polarization S parameter for e-Bi scattering at: (a) 11.0 eV, (b) 17.0 eV, (c) 24.0 eV, (d) 180.0 eV. Present calculations: (——) with real potential; (— — —) with complex potential, (— · — · —) calculations of Haberland and Fritsche [7]; (▲ ▲ ▲) experimental results of Kauseen *et al.* [26].

partial cross-sections. In the elastic region, the maximum of the cross-sections comes from p-wave whereas, near and beyond the inelastic threshold, d-wave makes the maximum contribution. The maxima in the d-wave cross-sections arise from shape resonance at energies E_r equal to 1.10 eV for Eu. The total cross-sections are also plotted in the figure under this model. Each curve shows a narrow low-energy maximum followed by sharp fall of the cross-sections up to the first inelastic threshold. Now turning our attention to Bi, as displayed in Figure 2b, it is seen that the total cross-section shows broad maxima at low energies and then falls off smoothly with the increase in the impact energies. The broad structure is due to the maxima in each of these s-, p- and d-wave partial cross-sections. Further, it is noted that for this case, the f-wave also contributes significantly to the total cross-sections beyond the first inelastic threshold.

2.4 Cross-sections and polarization parameters

Now, we present our elastic DCS and the S-parameter for electron scattering from Eu in Figures 3a–3d at energies 10.0, 50.0, 100.0 and 200.0 eV. Here we have presented our results for both real and complex potentials. It is seen that the present theory predicts the forward peaks, number of minima and maxima at middle angles and enhanced backward slopes of the DCS.

We further describe our results for angular distribution of the polarization of electrons scattered elastically from Bi atoms at 11.0, 17.0, 24.0 and 180.0 eV. The results are shown in Figures 4a–4d along with the experimental

Table 2. Elastic ($\sigma_{\rm el}$), absorption ($\sigma_{\rm abs}$) and total ($\sigma_{\rm t}$) cross-sections in units of 10^{-16} cm^2 in SEP model with absorption effects. $\sigma'_{\rm el}$ is the elastic scattering cross-section without absorption effects.

	europium (Eu)				bismuth (Bi)			
energy (eV)	$\sigma'_{\rm el}$	$\sigma_{\rm el}$	$\sigma_{\rm abs}$	$\sigma_{\rm t}$	$\sigma'_{\rm el}$	$\sigma_{\rm el}$	$\sigma_{\rm abs}$	$\sigma_{\rm t}$
2.0	209.505	209.505	0.000	209.505	58.198	58.198	0.000	58.198
5.0	96.934	96.934	0.000	96.934	62.328	62.328	0.000	62.328
10.0	69.798	65.890	5.795	71.685	48.160	48.094	2.964	49.058
20.0	56.107	51.072	6.882	57.954	35.353	31.742	4.830	36.572
30.0	41.848	37.988	6.184	44.171	27.942	24.819	4.987	29.805
50.0	28.570	25.540	5.424	30.965	15.984	13.716	4.915	18.631
80.0	22.977	20.199	4.458	24.657	11.612	9.778	4.271	14.049
100.0	20.172	17.671	3.973	21.640	10.838	9.156	3.843	13.000
150.0	15.577	13.678	3.142	16.817	9.735	8.365	3.065	11.430
200.0	12.878	11.374	2.615	13.989	8.720	7.538	2.582	10.120
250.0	11.128	9.884	2.251	12.135	7.949	6.876	2.258	9.134
300.0	9.904	8.848	1.976	10.823	7.399	6.422	2.014	8.435
350.0	8.998	8.081	1.761	9.845	6.968	6.078	1.818	7.895
400.0	8.295	7.487	1.590	9.078	6.599	5.785	1.657	7.442
450.0	7.449	7.006	1.450	8.459	6.269	5.521	1.522	7.044
500.0	7.262	6.614	1.333	7.946	5.971	5.281	1.409	6.689

Table 3. Momentum transfer cross-section ($\sigma_{\rm m}$) in units of 10^{-16} cm^2 for electron scattering from Eu and Bi atoms.

	Eu		Bi	
energy (eV)	SEP	SEPa	SEP	SEPa
2.0	89.833	89.833	47.238	47.238
5.0	57.520	57.520	33.766	33.766
10.0	27.155	24.352	14.918	13.643
20.0	10.771	8.666	6.944	5.488
30.0	9.467	5.262	9.525	7.034
50.0	5.781	4.263	8.251	5.626
80.0	2.570	1.809	4.724	3.047
100.0	1.949	1.350	3.720	2.417
150.0	1.547	1.067	2.462	1.670
200.0	1.499	1.056	1.785	1.234
250.0	1.471	1.061	1.447	1.005
300.0	1.426	1.053	1.296	0.909
350.0	1.366	1.028	1.223	0.871
400.0	1.299	0.994	1.178	0.852
450.0	1.228	0.955	1.141	0.839
500.0	1.158	0.910	1.107	0.825

data of Kaussen *et al.* [26] and the theoretical results of Haberland and Fritsche [7] employing *ab initio* calculations in a non-local exchange approximation based on Kohn and Sham method. The extreme value of the polarization as measured by Kaussen *et al.* [26] for Bi is much weaker compared to other targets like Hg, Tl and Pb. As pointed out there, the energy-loss spectrum with Bi target shows a strong influence of Bi_2 molecules, resulting in intramolecular multiple scattering, which brings changes in the measurement of polarization from this target. On comparison, we find that the general features of the angular dependence of the polarization parameter S of the present calculation are completely different from those of the experimental data [26] and the calculated values of Haberland and Fritsche [7] at lower impact energies. The changes in S values are very large over a wide range of scattering angles in particular at maxima and minima. Further, the situation is also not very different at high impact energies, however these differences narrow down. On the other hand, the theoretical results of Haberland and Fritsche [7] describe the general structure of the polarization curve quite well over the whole energy range of measurement. It is worth while to point out that the pronounced differences between the S parameter of the two sets of calculations must be the result of using different potentials in the formulation. We have done a compilation of the integrated elastic cross-sections with absorption effects ($\sigma_{\rm el}$) and without absorption effects ($\sigma'_{\rm el}$) together with absorption cross-section ($\sigma_{\rm abs}$) and total cross-section ($\sigma_{\rm t}$) in Table 2 for both Eu and Bi atoms. The momentum transfer cross-sections ($\sigma_{\rm m}$) for each of these atoms are presented in Table 3.

Finally, Figures 5a–5d present our results for T and U parameters at an incident energy of 200.0 eV for Eu and Bi atoms. As expected, there is an appreciable change about the magnitude of the maxima and minima, while their positions and width are only slightly modified.

3 Conclusions

In this paper, we have presented our relativistic theoretical results for different cross-sections and the angular variations of spin polarization parameters S, T and U for

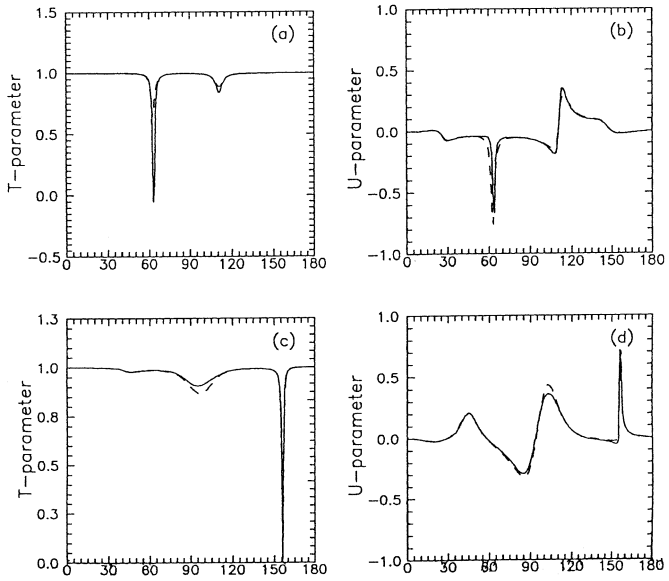

Fig. 5. Spin polarization parameters T and U at 200.0 eV for scattering of (a, b) e-Eu, (c, d) e-Bi. Present calculations: (——) with real potential; (— — —) with complex potential.

electrons scattered from Eu and Bi atoms at energies between 2.0 to 500.0 eV. Calculations have been done in two models; the first one includes a parameter free correlation polarization potential to account for the polarization of atomic charge cloud. The other model includes a phenomenological absorption potential to account for loss of electron flux into the non-elastic channels. Qualitatively the salient features (such as shape resonance phenomenon around 1.0 eV) in the cross-sections are reproduced by using this approach. Scattering of electron from these atoms shows significant amount of spin polarization in the scattered beam at various scattering angles. Obviously the fine-structure effect which is not included in this theory, alone is not responsible for the observed difference of the polarization curves. Accordingly, the differences may be due to different choices of the correcting potentials as well. This clearly indicates that there is a need for experimental measurements and other theoretical calculations in this energy region, so that it may provide a possibility of assessing accuracy of the present optical model.

The work was supported by the Board of Research in Nuclear Sciences (BRNS), Department of Atomic Energy, Govt. of India, India. One of the authors, Neerja, gratefully acknowledges the financial support.

References

1. N. Andersen, K. Bartschat, Adv. At. Mol. Phys. **36**, 1 (1996).
2. J. Kesslar, Adv. At. Mol. Opt. Phys. **27**, 81 (1991); see also *Polarized electrons*, 2nd edn. (Springer-verlag, Berlin, 1985).
3. G.F. hanne, Phys. Rep. **95**, 95 (1983).
4. K. Blum, *Density matrix Theory and Application* (Plenum, New York, 1981).
5. D.W. Walker, Adv. Phys. **20**, 257 (1971); J. Phys. B: At. Mol. Phys. **2**, 356 (1969).
6. L. Sin Fai Lam, J. Phys. B **15**, 119 (1982).
7. R. Haberland, L. Fritsche, J. Phys. B: At. Mol. Phys. **20**, 121 (1987).
8. K. Bartschat, H.J. Goerss, R.P. Nordbeck, Z. Phys. D **17**, 25 (1990).
9. K. Bartschat, J. Phys. B **20**, L 815 (1987).
10. R.P. McEachran, A.D. Stauffer, J. Phys. B **19**, 3523 (1986).
11. S.N. Nahar, J.M. Wadehra, Phys. Rev. A **43**, 1275 (1991); see also S.N. Nahar, J.M. Wadehra **35**, 2051 (1987).
12. P. Kumar, A.K. Jain, A.N. Tripathi, S.N. Nahar, Phys. Rev. A **49**, 899 (1994).
13. J. Yuan, Z. Zhang, Phys. Lett. A **168**, 291 (1992); Phys. Lett. A **160**, 181 (1991).
14. R. Szmytkowski, J. Phys. B: At. Mol. Opt. Phys. **24**, 3895 (1991); J. Phys. B: At. Mol. Opt. Phys. **26**, 535 (1993).
15. R. Szmytkowski, J.E. Sienkiewicz, J. Phys. B: At. Mol. Opt. Phys. **27**, 2277 (1994); Phys. Rev. A **50**, 4007 (1994).
16. J.E. Sienkiewicz, W.E. Baylis, Phys. Rev. A **55**, 1108 (1997).
17. A. Dorn, A. Elliot, J. Lower, S.F. Mazevet, R.P. McEachran, I.E. McCarthy, E. Weigold, J. Phys. B: At. Mol. Opt. Phys. **31**, 547 (1998).
18. Neerja, A.N. Tripathi, A.K. Jain, Phys. Rev. A **61**, 032713 (2000).
19. H.A. Bethe, R. Jackiw, *Intermediate Quantum Mechanics*, 2nd edn. (The Benjamin/Cummings publishing company, Ca, USA, 1968), p. 68.
20. A.D. McLean, R.S. McLean, At. Data Nucl. Data Table **26**, 197 (1981).
21. F. Salvat, J.D. Martinez, R. Mayol, J. Parellada, Phys. Rev. A **36**, 467 (1987) and references therein.
22. F.A. Gianturco, S. Scialla, J. Phys. B: At. Mol. Opt. Phys. **20**, 3171 (1987).
23. J.K. O'Connell, N.F. Lane, Phys. Rev. A **27**, 1893 (1983).
24. G. Staszewska, D.W. Schwenke, D.G. Truhlar, Phys. Rev A **29**, 3078 (1984).
25. P.G. Burke, *Potential Scattering in Atomic Physics* (Plenum, New York, 1977).
26. F. Kauseen, H. Geesmann, G.F. hanne, J. Kessler, J. Phys. B: At. Mol. Opt. Phys. **20**, 151 (1987).